HHS Public Access

Author manuscript

Organometallics. Author manuscript; available in PMC 2022 January 11.

Published in final edited form as:

Organometallics. 2021 January 11; 40(1): 72–82. doi:10.1021/acs.organomet.0c00728.

Fluorinated Cycloplatinated(II) Complexes Bearing Bisphosphine Ligands as Potent Anticancer Agents

Hamid R. Shahsavari

Department of Chemistry, Institute for Advanced Studies in Basic Sciences (IASBS), Zanjan, 45137-66731, Iran; Department of Chemistry and Biochemistry, University of Arkansas, Fayetteville, Arkansas, 72701, United States;

Jiyun Hu[#],

Department of Chemistry and Biochemistry, University of Arkansas, Fayetteville, Arkansas, 72701, United States.

Samira Chamyani[#],

Department of Chemistry, Institute for Advanced Studies in Basic Sciences (IASBS), Zanjan, 45137-66731, Iran.

Yoshie Sakamaki[#],

Department of Chemistry and Biochemistry, University of Arkansas, Fayetteville, Arkansas, 72701, United States.

Reza Babadi Aghakhanpour,

Department of Chemistry, Institute for Advanced Studies in Basic Sciences (IASBS), Zanjan, 45137-66731, Iran;

Christopher Salmon

Department of Chemistry and Biochemistry, University of Arkansas, Fayetteville, Arkansas, 72701, United States.

Masood Fereidoonnezhad, **Ayyub Mojaddami**, **Parnian Peyvasteh**

Department of Medicinal Chemistry, Ahvaz Jundishapur University of Medical Sciences, Ahvaz, 61357-15794, Iran.

Hudson Beyzavi

Department of Chemistry and Biochemistry, University of Arkansas, Fayetteville, Arkansas, 72701, United States;

[#] These authors contributed equally to this work.

Corresponding Author: Hamid R. Shahsavari − Department of Chemistry, Institute for Advanced Studies in Basic Sciences (IASBS), Zanjan, 45137-66731, Iran; Department of Chemistry and Biochemistry, University of Arkansas, Fayetteville, Arkansas, 72701, United States; shahsavari@iasbs.ac.ir. Hudson Beyzavi − Department of Chemistry and Biochemistry, University of Arkansas, Fayetteville, Arkansas, 72701, United States; beyzavi@uark.edu. Masood Fereidoonnezhad − Department of Medicinal Chemistry, Ahvaz Jundishapur University of Medical Sciences, Ahvaz, 61357-15794, Iran; fereidoonnezhad-m@ajums.ac.ir.

Accession Codes

CCDC 2017468 contains the supplementary crystallographic data for this paper. These data can be obtained free of charge *via* www.ccdc.cam.ac.uk/data_request/cif, or by data_request@ccdc.cam.ac.uk, or by contacting The Cambridge Crystallographic Data Centre, 12 Union Road, Cambridge CB2 1EZ, UK; fax: +44 1223 336033.

The authors declare no competing financial interest.

Abstract

A family of cationic cycloplatinated(II) complexes [Pt(dfppy)(P^P)]Cl, dfppy = 2-(2,4-difluorophenyl)pyridine, incorporating bisphosphine ligands, P^P = bis(diphenylphosphino)methane (**1**, dppm), 1,2-bis(diphenylphosphino)ethane (**2**, dppe) and 1,2-bis(diphenylphosphino)benzene (**3**, dppbz), was prepared. The complexes were characterized by means of several analytical and spectroscopic methods. These complexes displayed acceptable stability in the biological environments which was confirmed by NMR, HR ESI-MS and UV-vis techniques. The antiproliferative properties of these complexes were evaluated by National Cancer Institute (NCI) at National Institutes of Health (NIH) against 60 different human tumor cell lines such as leukemia, melanoma, lung, colon, brain, ovary, breast, prostate and kidney. These complexes showed higher cytotoxicity than cisplatin against a wide variety of cancer cell lines such as K-562 (leukemia), HOP-92 (lung), HCT-116 (colon), OVCAR-8 (ovarian), PC-3 (prostate), MDA-MB-468 (breast), and melanoma cancer cell lines. Complex **3** as the most potent compound in this study furnished an excellent anti-proliferative activity compared to the cisplatin against Hela, SKOV3, and MCF-7 cancer cell lines. The main mode of the interaction of **1–3** with DNA was also determined using molecular docking studies.

Graphical Abstract

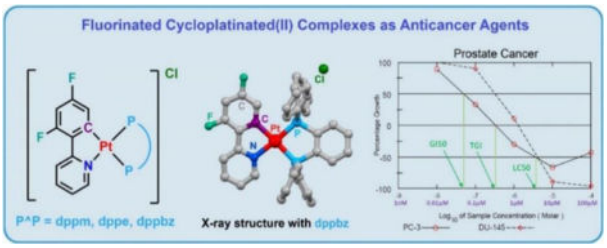

Introduction

Cisplatin, carboplatin and oxaliplatin are among the most well-known chemotherapeutic agents in the world.[1–5] These drugs interact with DNA *via* the formation of a coordinate bond between the Pt(II) center and the N7 of guanine in the DNA helix, leading to apoptototic cell death. Therefore, the dissociation of anionic ligand on Pt(II) center and the formation of Pt-DNA adduct significantly affect the performance of the drug.[6–8] In recent years, some new metal-based drugs such as pyriplatin, imidazoplatin and phenanthriplatin were developed and their activities were examined against some tumor cells.[1, 2, 9–11] These compounds demonstrated much higher cellular accumulation in comparison to the current anticancer agents. In spite of numerous investigations on Pt-based chemotherapeutic agents, several unsolved questions remain on the toxicity, ototoxicity, low selectivity, and drug resistance of cells.[12] To remove such limitations, many strategies have been employed such as using chelating ligands instead of Cl ligands,[13, 14] encapsulating agents to enhance drug delivery,[1, 15, 16] replacing of Pt(II) centers with Pt(IV) counterparts,[17–22] and using ligands which are able to selectively interact with biological targets.[23–29] Additionally, in order to achieve the best formulation for such drugs, their size, shape, and a favorable balance between lipophilicity and hydrophilicity should be considered. Thus, to facilitate the

administration and cell uptake for the drugs, the existence of lipophilic and hydrophilic functional groups seems to be necessary.[30]

Cycloplatinated(II) complexes are special kind of organoplatinum(II) complexes which exhibit attractive biological properties. Most of the investigations on anticancer properties of these compounds are attributed to the complexes which are bearing C^N ligands as the cyclometalated backbone.[31–45] The chelating nature of the C^N ligand and the strong Pt−C bond in these complexes warrant their stability in physiological conditions for reaching the target cells without any ligand disassociation. Moreover, the high *trans* influence of the C− ligating atom enhances the labiality of its *trans* ligand as a desirable leaving group.[17, 32, 46] In this regard, many studies demonstrated that the aromatic rings of cycloplatinated(II) complexes causes the intercalation of the complexes with the base pairs of DNA through non-covalent π···π stacking interactions.[47–50] In addition to the key role of the cyclometalated ligand, the biological properties of these complexes can be tuned by ancillary ligands.[31, 33–35, 38, 51, 52] In order to synthesize such therapeutic agents, mono and bisphosphine ligands are appropriate auxiliary ligands which were frequently employed in the structures of cyclometalated and non-cyclometalated Pt(II) complexes.[46, 53–59] The incorporating of phosphine ligands enhances the lipophilicity of cycloplatinated(II) complexes, resulting in high cytotoxicity of these compounds.[55, 60, 61] It was demonstrated that the cationic cyclometalated platinum(II) complexes with bisphosphines have significant potency against adenocarcinoma cell lines with higher activity than cisplatin.[55] Along with the phosphine ligands, the fluoro substituent was introduced as an excellent choice to modify the electronic properties and hydrophobicity of the Pt-based therapeutic agents and its role in medicinal chemistry is evidently obvious.[62–64]

Based on our experiences in the field of cycloplatinated(II) anticancer drugs,[31, 34, 38, 51, 65] herein, a series of cationic cycloplatinated(II) complexes including fluorinated cyclometalated ligand and different bisphosphine ancillary ligands were designed, synthesized, and characterized. The biological activities of these complexes were tested by us and National Cancer Institute (NCI) at National Institutes of Health (NIH). The NCI-60 Human Tumor Cell Lines Screen (NCI-60-HTCLS) has served the global cancer research community for over 20 years. The screening utilizes 60 different human tumor cell lines, representing leukemia, melanoma, lung, colon, brain, ovary, breast, prostate and kidney cancers to identify and characterize novel compounds with growth inhibition of tumor cell lines.

Results and Discussion

Synthesis and Characterization

The synthetic route for the new complexes is depicted in Scheme 1. The known precursor complex [Pt(dfppy)(dmso)Cl], **A**, dfppy = 2-(2,4-difluorophenyl)pyridine, was prepared by the reaction of K_2PtCl_4 with 2.5 eq. of dfppyH ligand[66] followed by dimethyl sulfoxide (dmso) treatment.[67] Then, **A** was reacted with three different diphosphine ligands to give a series of bis-chelated complexes [{Pt(dfppy)(P^P)}Cl], P^P = bis(diphenylphosphino)methane (**1**, dppm), 1,2-bis(diphenylphosphino)ethane (**2**, dppe), and 1,2-bis(diphenylphosphino)benzene (**3**, dppbz). The new complexes were characterized by

analytical (HR ESI-Mass and elemental analysis) and spectroscopic (NMR) methods. In order to ensure about the proposed structures, **3** has been further characterized by single crystal X-ray crystallography technique.

The NMR spectra of **1–3** are shown in the Figures 1 and S1–S9; however, details of **3** are discussed here as an example. In the ^{1}H NMR spectrum of **3** (Figure S9), the aromatic protons $H^{5'}$ and H^{6} appear as two multiplets with Pt satellites at δ 6.57 ppm ($^{3}J_{PtH}{}^{5'}$ = 63.1 Hz) and 8.34 ppm ($^{3}J_{PtH}{}^{6}$ = 26.7 Hz), respectively, which indicates the coordination of the dfppy ligand to the Pt(II) center as a chelate. The multiplet signal at δ 6.53 ppm is assigned to $H^{3'}$ which coupled with two aromatic F substituents and $H^{5'}$ of dfppy ligand. The broad doublet signal at δ 8.29 ppm is attributed to the H^{3} which shifts to downfield due to the hydrogen bonding interaction with $F^{2'}$ (the distance of H···F is 2.183 Å as determined from the single crystal structure). Two triplet signals at δ 7.02 ppm and 8.08 ppm is assigned to H^{5} and H^{4} protons of dfppy ligand, respectively. The ^{19}F{^{1}H} NMR spectra of **3** shows two different resonances which flanked by Pt satellites (Figure 1a). A doublet of doublet signal at δ −105.6 ppm is assigned to the $F^{4'}$ with $^{4}J_{PtF}{}^{4'}$ = 53 Hz. In this signal, the large and small doublets are corresponded to the coupling of $F^{4'}$ with $F^{2'}$ ($^{3}J_{F}{}^{2'}{}_{F}{}^{4'}$ = 11 Hz) and P^{b} ($^{5}J_{PtP}{}^{b}$ = 6 Hz), respectively. The signal of $F^{2'}$ substituent is observed as a triplet at δ −106.7 with Pt satellites ($^{4}J_{PtF}{}^{2'}$ = 41 Hz) which is coupled to $F^{4'}$ ($^{3}J_{F}{}^{2'}{}_{F}{}^{4'}$ = 11 Hz). The ^{31}P{^{1}H} NMR spectrum of **3** exhibits P^{a} and P^{b} of dppbz ligand at δ 36.1 ppm and 47.9 ppm, respectively, both having Pt satellites with $^{1}J_{PtP}{}^{a}$ = 3653 Hz and $^{1}J_{PtP}{}^{b}$ = 1896 Hz, respectively (Figure 1b). Because of the higher *trans* influence of C ligating atom of dfppy than N_{dfppy}, the Pt−P^{b} bond is longer than that of Pt−P^{a} and consequently the value of $^{1}J_{Pt\text{-}P}{}^{b}$ is considerably smaller in comparison of $^{1}J_{Pt\text{-}P}{}^{a}$. Since P^{a} is almost located at the *cis* position of F atoms of dfppy, it does not show any coupling with F atoms whereas the resonance of P^{b} shows a pseudo triplet pattern due to the coupling with two F atoms (see the inset in Figure 1b). The ^{195}Pt{^{1}H} NMR spectrum of **3** contains a doublet of doublet signal at δ −4529 ppm, due to the coupling with P^{a} and P^{b} atoms (Figure 1c).

The HR ESI-Mass spectra of **1–3** are recorded in positive mode and they demonstrate the high intense molecular peak associated with the $[M - Cl]^{+}$ fragment which are superimposable to the simulated pattern (Figures S10–S12). The crystal structure of **3** is confirmed by X-ray diffraction and its ORTEP drawing is shown in Figure 2. The structure of **3** is relatively deviated from its perfect square planar, because of the torsion angle (5.09°) between dfppy and benzene of dppbz planes. Also, the bite angels of C^N (C7-Pt1-N1) and P^P (P1-Pt1-P2) chelates are 79.69° and 85.72°, respectively, being much smaller than 90°. As mentioned in the ^{31}P{^{1}H} NMR discussion, due to the higher *trans* influence of coordinated carbon atom of dfppy than nitrogen ligating atom, the Pt1-P1 bond (*trans* to C, 2.3054(11) Å) is considerably longer than that of Pt1-P2 (*trans* to N, 2.2342(11) Å). A strong intramolecular hydrogen bonding can be observed between H4 of pyridyl ring and F1 on phenyl ring. The **π**···**π** (between two dfppy ligands, 3.396 Å, as a head-to-tail fashion) and C–H···**π** (between C−H of phenyl rings of dppbz and dfppy) interactions are observed in the crystal packing of **3** (Figure S13).

Biological Properties

The stability of the cycloplatinated(II) complexes was assessed before *in vitro* studies. ^{1}H, ^{19}F{^{1}H}, and ^{31}P{^{1}H} NMR spectroscopies showed that **1−3** were stable for at least 96 hours in dmso-d_6 (Figures S14−S22). UV-vis spectroscopy confirmed the stability of complexes in dmso solution over 96 h (Figures S26−S28). In addition, HR ESI-MS further demonstrated the intact coordination environment of **1−3** after being kept in water for 48 hours (Figures S23−S25).

The *in vitro* cytotoxic activities of **1–3** were evaluated against three human cancer cell lines including cervical (Hela), ovarian (SKOV3), and breast (MCF-7) carcinoma as well as a non-tumoral cell line (MCF-10A; normal human epithelial breast cell line). As presented in Table 1, all the synthesized complexes **1–3** showed higher anti-proliferative activity than cisplatin on the studied cell lines. For example, **3** as the most potent compound in this study showed an excellent anti-proliferative activity with IC_{50} of 0.135, 0.092, and 0.073 μM compared to those assessed for cisplatin which were 17.369, 13.733, and 12.372 μM against Hela, SKOV3, and MCF-7 cell lines, respectively.

In addition, in order to check the selectivity between cancer and normal cell line, the effects of these compounds on the proliferation of MCF-10A were also determined based on the procedure of our reported work.[68] As summarized in Table1, all of these compounds displayed fair selectivity between tumorigenic and non-tumorigenic cell lines. The selectivity index (SI) which represents IC_{50} for normal breast cell line/IC_{50} for cancerous breast cell line after 48 hours is shown in Table 1. All of these compounds showed better selectivity index compared to cisplatin.

On the other hand, the cycloplatinated complexes **1–3** were at least tested twice by the National Institutes of Health-60 Human Tumor Cell Lines Screen (NCI-60-HTCLS). First a single concentration is tested in all 60 cell lines at a single dose of 10^{-5} M. All compounds satisfying pre-determined threshold inhibition criteria in a minimum number of cell lines and therefore, were selected for further five dose assays by NCI. The five-dose assay gave drug response curves. Three endpoints on the dose response curves were calculated. For instance, Figure 3 shows data of **1** for prostate cancer cell lines. The synthesized compounds were evaluated at five concentrations (1 log dilutions from 10^{-8} M to 10^{-4} M). In the process of the assay, a growth rate of 100 corresponds to the growth seen in untreated cells and a growth rate of 0 does not imply any net growth. (*i.e.* equals the number of time zero cells). The death of all cells after treatment is denoted by a growth rate of −100. Three endpoints are calculated regularly: 1) GI_{50}, log M concentration resulting in 50 growth rate (*i.e.* 50% growth inhibition), 2) TGI, log M concentration resulting in 0 growth rate, or total growth inhibition, and 3) LC_{50}, log M concentration that yields a growth percentage of −50 or 50% lethality of the starting cell. As shown in Figure 3, these endpoints are illustrated for cell line PC-3(red open circle). The other cell line displayed was DU-145 (red open diamond). All the results from NCI-60-HTCLS on **1–3** are shown in Figures 4, S29 and S30, while the original number data are shown in Figures S31–S33.

These complexes showed their ability to inhibit the growth of the majority of cancerous cells in NCI-60-HTCLS at concentration of 10 μM. Each complex's GI_{50}, TGI, and LC_{50} in

NCI-60-HTCLS are presented in Figures S34–S36. The difference between the GI_{50} for a particular cell line and the mean GI_{50} is plotted here. Cell lines that were more sensitive are displayed as bars that project to the right of the mean (Figures S34–S36). Cell lines that were less sensitive are displayed with bars projected to the left (Figures S34–S36). Leukemia cell lines such as HL-60, K-562, and SR, melanoma cell line such as MALME-3M, prostate cancer cell lines such as PC-3, and breast cancer cell lines such as T-47D are more sensitive when exposed to **1** (Figure S34). Non-small cell lung cancer except HOP-92, ovarian, colon, CNS, and renal cancer cell lines are less sensitive to **1**. As presented in Figure S35, leukemia cell lines such as HL-60, K-562, and SR, CNS cancer cell lines such as SF-295, SNB-19, SNB-75, and U251, prostate cancer cell lines, and breast cancer cell lines such as MCF-7, MDA-MB-468, and T-47D are more sensitive when exposed to **2**. Non-small cell lung cancer except A549, melanoma cancer cell lines except MALME-3M, ovarian cancer cell lines except OVCAR-8, colon cell lines except HCT-116, and renal cell lines except SN120 are less sensitive to **2**. The effect of **3** on the growth inhibition of all the studied cancer cell lines are shown in Figure S36. Leukemia cell lines, CNS cancer cell lines, prostate cancer cell lines, and breast cancer cell lines such as MDA-MB-468, and T-47D are more sensitive when exposed to **3**. Non-small cell lung cancer except A549, melanoma cancer cell lines except MALME-3M, ovarian cancer cell lines except OVCAR-8, colon cancer cell lines except HCT-116, and renal cell lines except SN120 are less sensitive to **3**. These complexes showed better cytotoxicity against cisplatin-resistant cell lines such as K-562 (leukemia), HOP-92 (lung), HCT-116 (colon), OVCAR-8 (ovarian), PC-3 (prostate), MDA-MB-468 (breast), and melanoma cancer cell lines.

As shown in Table 2, the mean GI_{50}, TGI, and LC_{50} values across all cell lines in NCI-60-HTCLS are calculated for **1–3**. The dose-response curve and values for cisplatin in NCI-60-HTCLS are available on NCI-60-HTCLS data source (NSC number: 119875, Figure S37–S40) and are compared to **1–3**.[69] The mean values of cisplatin is described in Table 2 as reference for **1–3**.

These complexes show 10 times smaller LC_{50} than cisplatin, which indicates that our new synthesized cycloplatinated(II) complexes are 10 times more effective than cisplatin to a variety of cancer cell lines. In addition, cisplatin has no cell growth inhibitory effect on central nervous system cancer (CNS), whereas **1–3** significantly inhibit the growth of CNS cancer cells (Figures 4, S29, S30 and S37). Among the synthesized compounds, **3** shows higher cytotoxicity against the studied cancer cell lines.

Molecular Docking

Main mode of action of cisplatin has been proposed to be *via* covalent binding to DNA.[70] In order to determine the binding mode of **1**–**3** to DNA, molecular docking was conducted. As we previously reported,[38] two of the most widely found modes of interaction of platinum anticancer agents with the DNA are DNA groove binding (in the major or minor groove of the DNA), and DNA intercalation. In groove binding mode, the ligand is usually versatile, contains rotatable bonds, and is able to align itself along the DNA's major or minor groove of the DNA, thus inhibiting normal DNA function. The DNA intercalators, on the other

hand, are usually inflexible planar molecules that stack between the base pairs of DNA allowing an intercalation gap in the helical structure of DNA.

Molecular docking revealed the binding modes and the best binding energies of these Pt(II) complexes to DNA. The best docking binding energies are −8.56, −8.10 and −8.72 kcal.mol $^{-1}$ for **1**–**3**, respectively. These negativity values of free binding energy (ΔG_{bind}), showed that these complexes reasonably bind to the DNA but in a non-covalently manner (Figures 5 and 6). The docking model suggests that the docking pose of **1** interacts with the minor groove of 3CO3 (Figure 5A). The dppm ligand of this complex fits into the minor groove of the DNA and participate in hydrophobic interactions with the base pairs in the minor groove and the dfppy group placed away from the gap. Also, **2** interacts with the base pairs in the major groove of the DNA through the hydrophobic interactions of dfppy moiety and the dppe group placed away from the gap (Figure 5B). The docking model suggests that **3** interacts with the major groove of 3CO3 (Figure 6). It interacts through dipole-dipole interaction *via* phosphorus atoms of dppbz ligand with G7 and A8 base pairs inside the DNA major groove.

Conclusion

The present study investigates the synthesis of a series of cationic bis-chelated cycloplatinated(II) complexes containing dfppy and bisphosphine chelating ligands (dppm, dppe, dppbz). The complexes were characterized by means of different spectroscopic methods. The complex containing dppbz, **3**, was further characterized with X-ray crystallography technique, confirming the bis-chelated structure of this complex. Based on the NMR, HR ESI-MS and UV-vis assessment the cycloplatinated complexes **1–3** exhibited good stability in the physiological media. The synthesized cycloplatinated(II) complexes are 10 times more effective than cisplatin against a wide variety of cancer cell lines. In addition, **1–3** significantly inhibit the growth of central nervous system cancer (CNS) cancer cells, whereas cisplatin has no cell growth inhibitory effect on CNS. These complexes showed better cytotoxicity against cisplatin-resistant cell lines such as K-562 (leukemia), HOP-92 (lung), HCT-116 (colon), OVCAR-8 (ovarian), PC-3 (prostate), MDA-MB-468 (breast), and melanoma cancer cell lines. Among the synthesized compounds, **3** showed higher cytotoxicity against the studied cancer cell lines. Complex **3** showed an excellent and clearly better anti-proliferative activity than cisplatin, with IC_{50} of 0.135, 0.092, and 0.073 μM against Hela, SKOV3, and MCF-7 cell lines, respectively. The main mode of the interaction of these compounds with DNA was also determined using molecular docking studies, which revealed that these complexes reasonably bind to the DNA in a non-covalently manner, mainly through the hydrophobic interactions with the base pairs in the minor and major groove of the DNA. These compounds have the potential to be very effective in the future of cancer treatment.

Experimental Section

General procedures and materials

^{1}H NMR (400 MHz), ^{19}F{^{1}H} (376 MHz), ^{31}P{^{1}H} NMR (162 MHz) and ^{195}Pt{^{1}H} (86 MHz) spectra were recorded on a Bruker Avance instrument at 295 K. All chemical shifts

(δ) are reported in ppm relative to their corresponding external standards ($SiMe_4$ for ^1H, $CFCl_3$ for $^{19}F\{^1H\}$, 85% H_3PO_4 for $^{31}P\{^1H\}$, Na_2PtCl_6 for $^{195}Pt\{^1H\}$) and the coupling constants (*J*) have being expressed in Hz. The instrument for HR ESI-Mass measurement was a Shimadzu IT-TOF with an electrospray ionization source, which is part of the Arkansas Statewide Mass Spectrometry Facility. The 2-(2,4-difluorophenyl)pyridine (dfppy), bis(diphenylphosphino)methane (dppm), 1,2-bis(diphenylphosphino)ethane (dppe) and 1,2-bis(diphenylphosphino)benzene (dppbz) and all the other chemicals were purchased from commercial resources. All the reactions were carried out under Argon atmosphere and in the common solvents and all solvents were purified and dried according to standard procedures.[71] The complexes [Pt(dfppy)(dfppyH)Cl][66] and [Pt(dfppy)(dmso)Cl], **A**,[67] were prepared as published methods. The NMR labeling is shown in Scheme 1 for clarifying the chemical shift assignments.

[{Pt(dfppy)(dppm)}Cl], 1—To a solution of **A** (100 mg, 0.2 mmol) in acetone (15 mL) was added dppm ligand (77 mg, 0.2 mmol). The reaction mixture was stirred for 3 h at room temperature, then the solvent was concentrated to a small volume (~ 2 mL) and *n*-hexane (5 mL) was added to precipitate **1** as a greenish solid. Yield: 83% (134 mg, 0.17 mmol). HR ESI-MS(+) m/z Cacld. for $C_{36}H_{28}F_2NP_2Pt$ $[M-Cl]^+$ 769.1310; Found 769.1287. Elem. Anal. Calcd for $C_{36}H_{28}ClF_2NP_2Pt$ (805.09): C, 53.71; H, 3.51; N, 1.74; Found: C, 53.64; H, 3.52; N, 1.79. ^1H NMR (400 MHz, $CDCl_3$, 295 K): δ 8.44 (m, 1H, H^6), 8.29 (d, $^3J_{HH}$ = 8.2 Hz, 1H, H^3), 8.07 (t, $^3J_{HH}$ = 8.3 Hz, 1H, H^4), 7.93–7.76 (m, 8H, H^o, Ph), 7.55–7.46 (m, 12H, H^m and H^p, Ph), 7.23 (t, $^3J_{HH}$ = 6.4 Hz, 1H, H^5), 6.57 (m, 1H, $H^{3'}$), 6.46 (m, $^3J_{PtH}{}^{5'}$ = 59.7 Hz, 1H, $H^{5'}$), 5.09 (m, 2H, CH_2 of dppm); ^{19}F NMR (376 MHz, $CDCl_3$, 295 K): δ −105.1 (m, $^4J_{PtF}$ = 48 Hz, 1F, $F^{4'}$), −107.2 (m, $^4J_{PtF}$ = 40 Hz, 1F, $F^{2'}$); $^{31}P\{^1H\}$ NMR (162 MHz, $CDCl_3$, 295 K): δ −27.1 (m, $^1J_{PtP}$ = 1501 Hz, 1P, P^b), −34.8 (s, $^1J_{PtP}$ = 3293 Hz, 1P, P^a); $^{195}Pt\{^1H\}$ NMR (86 MHz, $CDCl_3$, 295 K): δ −3962 (dd, $^1J_{PtP}$ = 3292 Hz, $^1J_{PtP}$ = 1506 Hz, 1Pt).

The other complexes were made similarly using **A** and the appropriate bis phosphine ligands.

[{Pt(dfppy)(dppe)}Cl], 2—Yield: 92% (151 mg, 0.18 mmol). HR ESI-MS(+) m/z Cacld. for $C_{37}H_{30}F_2NP_2Pt$ $[M-Cl]^+$ 783.1467; Found 783.1448. Elem. Anal. Calcd for $C_{37}H_{30}ClF_2NP_2Pt$ (819.12): C, 54.25; H, 3.69; N, 1.71; Found: C, 54.34; H, 3.73; N, 1.69. ^1H NMR (400 MHz, $CDCl_3$, 295 K): δ 8.31 (d, $^3J_{HH}$ = 8.1 Hz, 1H, H^3), 8.26 (m, $^3J_{PtH}$ = 28.4 Hz, 1H, H^6), 8.02 (t, $^3J_{HH}$ = 8.0 Hz, 1H, H^4), 7.92–7.79 (m, 8H, H^o, Ph), 7.60–7.51 (m, 12H, H^m and H^p, Ph), 6.93 (t, $^3J_{HH}$ = 6.9 Hz, 1H, H^5), 6.53 (m, $^3J_{PtH}{}^{5'}$ = 62.6 Hz, 2H, $H^{3'}$ and $H^{5'}$), 2.76–2.52 (m, 4H, CH_2 of dppe); ^{19}F NMR (376 MHz, $CDCl_3$, 295 K): δ −105.7 (dd, $^4J_{PtF}$ = 51 Hz, $^3J_{FF}$ = 11 Hz,$^5J_{PtP}$ = 7 Hz, 1F, $F^{4'}$), −106.9 (t, $^4J_{PtF}$ = 45 Hz, $^3J_{FF}$ = 11 Hz, 1F, $F^{2'}$); $^{31}P\{^1H\}$ NMR (162 MHz, $CDCl_3$, 295 K): δ 50.7 (t, $^1J_{PtP}$ = 1920 Hz, $^5J_{PtP}$ = 7 Hz, 1P, P^b), 36.1 (s, $^1J_{PtP}$ = 3671 Hz, 1P, P^a); $^{195}Pt\{^1H\}$ NMR (86 MHz, $CDCl_3$, 295 K): δ −4573 (dd, $^1J_{PtP}$ = 3676 Hz, $^1J_{PtP}$ = 1922 Hz, 1Pt).

[{Pt(dfppy)(dppbz)}Cl], 3—Yield: 86% (149 mg, 0.17 mmol). HR ESI-MS(+) m/z Cacld. for $C_{41}H_{30}F_2NP_2Pt$ $[M-Cl]^+$ 831.1467; Found 831.1454. Elem. Anal. Calcd for $C_{41}H_{30}ClF_2NP_2Pt$ (867.16): C, 56.79; H, 3.49; N, 1.62; Found: C, 56.83; H, 3.46; N, 1.60.

^{1}H NMR (400 MHz, $CDCl_3$, 295 K): δ 8.34 (m, $^{3}J_{PtH}$ = 26.7 Hz, 1H, H^6), 8.29 (d, $^{3}J_{HH}$ = 7.8 Hz, 1H, H^3), 8.08 (t, $^{3}J_{HH}$ = 7.9 Hz, 1H, H^4), 7.74–7.38 (m, 24 H, H^a, H^b, H^c, H^d, H^o, H^m and H^p, Ph), 7.02 (t, $^{3}J_{HH}$ = 6.3 Hz, 1H, H^5), 6.57 (m, $^{3}J_{PtH}$ = 63.1 Hz, 1H, $H^{5'}$), 6.53 (m, 1H, $H^{3'}$); ^{19}F NMR (376 MHz, $CDCl_3$, 295 K): δ −105.6 (dd, $^{4}J_{PtF}$ = 53 Hz, $^{3}J_{FF}$ = 11 Hz,$^{5}J_{PtP}$ = 6 Hz, 1F, $F^{4'}$), −106.7 (t, $^{4}J_{PtF}$ = 41 Hz, $^{3}J_{FF}$ = 11 Hz, 1F, $F^{2'}$); ^{31}P{^{1}H} NMR (162 MHz, $CDCl_3$, 295 K): δ 47.9 (t, $^{1}J_{PtP}$ = 1896 Hz, $^{5}J_{PtP}$ = 6 Hz, 1P, P^b), 36.1 (s, $^{1}J_{PtP}$ = 3653 Hz, 1P, P^a); ^{195}Pt{^{1}H} NMR (86 MHz, $CDCl_3$, 295 K): δ −4529 (dd, $^{1}J_{PtP}$ = 3651 Hz, $^{1}J_{PtP}$ = 1897 Hz, 1Pt).

X-ray Crystallography

Single crystals of **3** were obtained by slow diffusion of *n*-hexane into its CH_2Cl_2 solution at room temperature. A colorless, needle-shaped crystal of dimensions 0.045 × 0.045 × 0.168 mm was selected for structural analysis. Intensity data for **3** were collected using a D8 Quest diffractometer with a Bruker Photon II ccd area detector[72, 73] and an Incoatec Iμs microfocus Mo Kα source (λ = 0.71073 Å). The sample was cooled to 100(2) K. Cell parameters were determined from a least-squares fit of 9023 peaks in the range 2.52 < θ < 24.13°. A total of 52618 data were measured in the range 2.321 < θ < 24.128° using ϕ and ω oscillation frames. The data were corrected for absorption by the empirical method[74] giving minimum and maximum transmission factors of 0.3948 and 0.4894. The data were merged to form a set of 6501 independent data with R(int) = 0.0334 and a coverage of 99.9 %.

The triclinic space group $P\bar{1}$ was determined by statistical tests and verified by subsequent refinement. The structure was solved by direct methods and refined by full-matrix least-squares methods on F^2.[75, 76] The positions of hydrogens were initially determined by geometry and were refined using a riding model. Non-hydrogen atoms were refined with anisotropic displacement parameters. Hydrogen atom displacement parameters were set to 1.2 times the isotropic equivalent displacement parameters of the bonded atoms. A total of 487 parameters were refined against 6501 data to give wR(F^2) = 0.0756 and S = 1.000 for weights of $w = 1/[\sigma^2 (F^2) + (0.0450\ P)^2 + 9.8000\ P]$, where $P = [F_o^2 + 2F_c^2] / 3$. The final R(F) was 0.0265 for the 6361 observed, [$F > 4\sigma(F)$], data. The largest shift/s.u. was 0.000 in the final refinement cycle. The final difference map had maxima and minima of 0.802 and −1.698 e/Å^3, respectively.

Biological Assay

Stability studies—NMR, mass and UV-vis measurements were carried out to check the stability of **1–3** in biological conditions. A solution of **1–3** (6 mg/mL) in dmso-d_6 was used for NMR experiments and the spectra were recorded in the appropriate sequences at room temperature. For mass experiments, **1–3** were dissolved in water and the MS spectra were recorded after 48 h. The UV-vis absorption spectra were recorded in the freshly prepared 2 × 10^{-5} M solutions of **1–3** in dmso.

Cytotoxic activity—The cytotoxic activities of the synthesized complexes were evaluated by National Cancer Institute (NCI) at National Institutes of Health (NIH) against 60 different human tumor cell lines. The details of experimental procedure is provided in the

Supporting Information based on the methodology presented by the by NCI (https://dtp.cancer.gov/discovery_development/nci-60/methodology.htm).

Determination the IC_{50} of the synthesized complexes using MTT assay—The human cancer cell lines, Hela (cervical cancer), SKOV3 (ovarian cancer), and MCF-7 (breast cancer) were grown in complete culture media containing RPMI 1640 (Biosera, France), 10% fetal bovine serum (FBS; Gibco, USA) and 1% penicillin-streptomycin (Biosera, France) and kept at 37 °C in a humidified CO_2 incubator. MCF10A cells (human breast epithelial cell line) were cultured in DMEM/Ham's F-12 (GIBCO-Invitrogen, Carlsbad, CA) supplemented with 100 ng/ml cholera toxin, 20 ng/ml epidermal growth factor (EGF), 0.01 mg/ml insulin, 500 ng/ml hydrocortisone, and 5% chelex-treated horse serum. A standard 3-(4,5-dimethylthiazol-yl)-2,5-diphenyl-tetrazolium bromide (MTT) assay has been used to determine the cytotoxic activities of complexes. To do this, the cells were seeded in 96-well microplates with a density of 0.8×10^4 cells per well and kept for 24h to recover. The cells were then treated in a triplicate manner with **1**–**3** at varying concentrations ranging from 0.01 to 100 μM and incubated in a humidified CO_2 incubator for at least 48 hours at 37 °C. The media was completely discarded after incubation and replaced with 150 μl of RPMI 1640 containing 0.5 mg/mL MTT solution and incubated for 3h at room temperature. The media containing MTT was discarded again to dissolve the formazan crystals and 150 μl of dmso was applied to each well and incubated in the dark for at least 30 min at 37 °C. The absorbance of individual well was then read by ELISA reader at 490 nm. CurveExpert 1.4 was used to measure the 50% inhibitory concentration of each compound, reflecting IC_{50}. The data are is given as mean ± Standard Deviation.

Molecular Docking—The docking simulations were performed using AutoDock 4.2[77] based on lamarchian genetic algoritm search method. Ligand and receptor preparation are two main steps in the molecular docking studies. For receptor preparation, the 3D crystal structure of DNA (PDB ID: 3CO3) was retrieved from protein data bank (www.rcsb.org/pdb). Then, co-crystal ligand molecules were excluded from the structure. By centering the grid box on the minor groove, major groove and the intercalation site to cover the complete DNA structure, the grid center on the DNA was retained. The grid maps were spaced 0.375 Å. All the other parameters were kept at their default values. Parameters for docking with metal ions such as platinum, used in the docking calculation have been added to gpf and dpf files.

For ligand preparation, the structure of **1–3** was created by HyperChem Professional (Version 8, Hypercube Inc., Gainesville, FL, USA). Then, they were optimized by molecular mechanic methods (MM^+) using HyperChem 8, followed by energy minimization calculations at Hartree-Fock (HF) level, using Gaussian 09.[78] The final structures of ligands were then converted to PDBQT using MGLtools 1.5.6. All calculations were performed with Windows 10 operating system on a core i7 personal computer (CPU at 8 MB). The lowest docking binding energy conformation was chosen as the best binding mode with respect to the AutoDock scoring features. The docked pose visualization was performed by means of AutoDock Tools 1.5.6 and and Molecular Operating Environment (MOE).[68]

Supplementary Material

Refer to Web version on PubMed Central for supplementary material.

Acknowledgment

H.B. gratefully acknowledges financial support through the startup funds from the University of Arkansas and NIHNIGMS (Grant GM132906). We thank Arkansas Statewide Mass Spectrometry Facility (NIH-NIGMS (Grant P30 GM103450)) for mass spectroscopy measurements reported in this paper. H.R.S. acknowledges the IASBS Research Council (Grant G2020IASBS32629) for his sabbatical leave at the University of Arkansas and Iran National Science Foundation (Grant 97007977). M.F. acknowledges the Department of Medicinal Chemistry, School of Pharmacy, Ahvaz Jundishapur University of Medical Sciences (B98035). We sincerely thank the National Cancer Institute Developmental Therapeutics Program (NCI/DTP, https://dtp.cancer.gov) as the source of *in vitro* data (NCI-60-HTCLS screening). The authors thank the National Science Foundation (grant CHE-1726630) and the University of Oklahoma for funds to purchase of the X-ray instrument and computers. The single crystal structure of **3** was determined by Dr. Douglas R. Powell.

References

1. Johnstone TC; Suntharalingam K; Lippard SJ, The Next Generation of Platinum Drugs: Targeted Pt(II) Agents, Nanoparticle Delivery, and Pt(IV) Prodrugs. Chem. Rev 2016, 116, 3436–3486. [PubMed: 26865551]
2. Wilson JJ; Lippard SJ, Synthetic Methods for the Preparation of Platinum Anticancer Complexes. Chem. Rev 2014, 114, 4470–4495. [PubMed: 24283498]
3. Mügge C; Marzo T; Massai L; Hildebrandt J; Ferraro G; Rivera-Fuentes P; Metzler-Nolte N; Merlino A; Messori L; Weigand W, Platinum(II) Complexes with O,S Bidentate Ligands: Biophysical Characterization, Antiproliferative Activity, and Crystallographic Evidence of Protein Binding. Inorg. Chem 2015, 54, 8560–8570. [PubMed: 26280387]
4. Dhar S; Gu FX; Langer R; Farokhzad OC; Lippard SJ, Targeted Delivery of Cisplatin to Prostate Cancer Cells by Aptamer Functionalized Pt(IV) Prodrug-PLGA–PEG Nanoparticles. Proc. Natl. Acad. Sci 2008, 105, 17356–17361. [PubMed: 18978032]
5. Farrell N, Multi-platinum Anti-cancer Agents. Substitution-inert Compounds for Tumor Selectivity and New Targets. Chem. Soc. Rev 2015, 44, 8773–8785. [PubMed: 25951946]
6. White JD; Haley MM; DeRose VJ, Multifunctional Pt(II) Reagents: Covalent Modifications of Pt Complexes Enable Diverse Structural Variation and In-cell Detection. Acc. Chem. Res 2016, 49, 56–66. [PubMed: 26641880]
7. Wang X; Guo Z, Targeting and Delivery of Platinum-based Anticancer Drugs. Chem. Soc. Rev 2013, 42, 202–224. [PubMed: 23042411]
8. Patra M; Johnstone TC; Suntharalingam K; Lippard SJ, A Potent Glucose–platinum Conjugate Exploits Glucose Transporters and Preferentially Accumulates in Cancer Cells. Angew. Chem. Int. Ed 2016, 128, 2596–2600.
9. Lovejoy KS; Todd RC; Zhang S; McCormick MS; D'Aquino JA; Reardon JT; Sancar A; Giacomini KM; Lippard SJ, *cis*-Diammine(pyridine)chloroplatinum(II), a Monofunctional Platinum(II) Antitumor Agent: Uptake, Structure, Function, and Prospects. Proc. Natl. Acad. Sci 2008, 105, 8902–8907. [PubMed: 18579768]
10. Park GY; Wilson JJ; Song Y; Lippard SJ, Phenanthriplatin, a Monofunctional DNA-binding Platinum Anticancer Drug Candidate with Unusual Potency and Cellular Activity Profile. Proc. Natl. Acad. Sci 2012, 109, 11987–11992. [PubMed: 22773807]
11. Johnstone TC; Wilson JJ; Lippard SJ, Monofunctional and Higher-valent Platinum Anticancer Agents. Inorg. Chem 2013, 52, 12234–12249. [PubMed: 23738524]
12. Ma J; Wang Q; Yang X; Hao W; Huang Z; Zhang J; Wang X; Wang PG, Glycosylated Platinum(IV) Prodrugs Demonstrated Significant Therapeutic Efficacy in Cancer Cells and Minimized Side-effects. Dalton Trans. 2016, 45, 11830–11838. [PubMed: 27373800]

13. Hartinger CG; Nazarov AA; Ashraf SM; Dyson PJ; Keppler BK, Carbohydrate-metal Complexes and their Potential as Anticancer Agents. Curr. Med. Chem 2008, 15, 2574–2591. [PubMed: 18855680]

14. Kenny RG; Chuah SW; Crawford A; Marmion CJ, Platinum(IV) Prodrugs–a Step Closer to Ehrlich's Vision? Eur. J. Inorg. Chem 2017, 2017, 1596–1612.

15. Vergaro V; Papadia P; Leporatti S; De Pascali SA; Fanizzi FP; Ciccarella G, Synthesis of Biocompatible Polymeric Nano-capsules Based on Calcium Carbonate: A Potential Cisplatin Delivery System. J. Inorg. Biochem 2015, 153, 284–292. [PubMed: 26560986]

16. Pontillo N; Pane F; Messori L; Amoresano A; Merlino A, Cisplatin Encapsulation within a Ferritin Nanocage: A High-resolution Crystallographic Study. Chem. Commun 2016, 52, 4136–4139.

17. Bauer E; Domingo X; Balcells C; Polat IH; Crespo M; Quirante J; Badía J; Baldomà L; Font-Bardia M; Cascante M, Synthesis, Characterization and Biological Activity of New Cyclometallated Platinum(IV) Iodido Complexes. Dalton Trans. 2017, 46, 14973–14987. [PubMed: 29048088]

18. Gabano E; Ravera M; Zanellato I; Tinello S; Gallina A; Rangone B; Gandin V; Marzano C; Bottone MG; Osella D, An unsymmetric Cisplatin-based Pt(IV) Derivative Containing 2-(2-Propynyl)octanoate: A Very Efficient Multi-action Antitumor Prodrug Candidate. Dalton Trans. 2017, 46, 14174–14185. [PubMed: 28984330]

19. Sommerfeld NS; Strohhofer D; Cseh K; Theiner S; Jakupec MA; Koellensperger G; Galanski M; Keppler BK, Platinum (IV) Complexes Featuring Axial Michael Acceptor Ligands–Synthesis, Characterization, and Cytotoxicity. Eur. J. Inorg. Chem 2017, 2017, 4049–4054.

20. Zhang P; Sadler PJ, Redox-active Metal Complexes for Anticancer Therapy. Eur. J. Inorg. Chem 2017, 2017, 1541–1548.

21. Yap SQ; Chin CF; Hong Thng AH; Pang YY; Ho HK; Ang WH, Finely Tuned Asymmetric Platinum(IV) Anticancer Complexes: Structure–Activity Relationship and Application as Orally Available Prodrugs. ChemMedChem 2017, 12, 300–311. [PubMed: 28028938]

22. Karmakar S; Chatterjee S; Purkait K; Mukherjee A, Anticancer Activity of a Chelating Nitrogen Mustard Bearing Tetrachloridoplatinum (IV) Complex: Better Stability Yet Equipotent to the Pt(II) Analogue. Dalton Trans. 2016, 45, 11710–11722. [PubMed: 27230464]

23. Martínez MA n.; Carranza MP; Massaguer A; Santos L; Organero JA; Aliende C; de Llorens R; Ng-Choi I; Feliu L; Planas M, Synthesis and Biological Evaluation of Ru(II) and Pt(II) Complexes Bearing Carboxyl Groups as Potential Anticancer Targeted Drugs. Inorg. Chem 2017, 56, 13679–13696. [PubMed: 29099179]

24. D'Errico S; Borbone N; Piccialli V; Di Gennaro E; Zotti A; Budillon A; Vitagliano C; Piccialli I; Oliviero G, Synthesis and Evaluation of the Antitumor Properties of a Small Collection of PtII Complexes with 7-Deazaadenosine as Scaffold. Eur. J. Org. Chem 2017, 2017, 4935–4947.

25. Muhammad N; Sadia N; Zhu C; Luo C; Guo Z; Wang X, Biotin-tagged Platinum(IV) Complexes as Targeted Cytostatic Agents Against Breast Cancer Cells. Chem. Commun 2017, 53, 9971–9974.

26. Liang H; Hao T; Yin C; Yang X; Fu H; Zheng X; Li R; Xiao D; Chen H, Cyclometalated Rhodium(III) Complexes Based on Substituted 2-Phenylpyridine Ligands: Synthesis, Structures, Photophysics, Electrochemistry, and DNA-Binding Properties. Eur. J. Inorg. Chem 2017, 4149–4157.

27. Nosova YN; Foteeva LS; Zenin IV; Fetisov TI; Kirsanov KI; Yakubovskaya MG; Antonenko TA; Tafeenko VA; Aslanov LA; Lobas AA, Enhancing the Cytotoxic Activity of Anticancer Pt^{IV} Complexes by Introduction of Lonidamine as an Axial Ligand. Eur. J. Inorg. Chem 2017, 2017, 1785–1791.

28. Medrano MA; Morais M; Ferreira VF; Correia JD; Paulo A; Santos I; Navarro-Ranninger C; Valdes AA; Casini A; Mendes F, Nonconventional *trans*-Platinum Complexes Functionalized with RDG Peptides: Chemical and Cytototoxicity Studies. Eur. J. Inorg. Chem 2017, 2017, 1835–1840.

29. Pages BJ; Garbutcheon-Singh KB; Aldrich-Wright JR, Platinum Intercalators of DNA as Anticancer Agents. Eur. J. Inorg. Chem 2017, 2017, 1613–1624.

30. Haghdoost M; Golbaghi G; Létourneau M; Patten SA; Castonguay A, Lipophilicity-antiproliferative Activity Relationship Study Leads to the Preparation of a Ruthenium(II) Arene Complex with Considerable In vitro Cytotoxicity Against Cancer Cells and a Lower In vivo

Toxicity in Zebrafish Embryos than Clinically Approved Cisplatin. Eur. J. Med. Chem 2017, 132, 282–293. [PubMed: 28371640]

31. Fereidoonnezhad M; Niazi M; Shahmohammadi Beni M; Mohammadi S; Faghih Z; Faghih Z; Shahsavari HR, Synthesis, biological evaluation, and molecular docking studies on the DNA binding interactions of platinum(II) rollover complexes containing phosphorus donor ligands. ChemMedChem 2017, 12, 456–465. [PubMed: 28195406]
32. Babak MV; Pfaffeneder-Kmen M; Meier-Menches SM; Legina MS; Theiner S; Licona C; Orvain C; Hejl M; Hanif M; Jakupec MA, Rollover Cyclometalated Bipyridine Platinum Complexes as Potent Anticancer Agents: Impact of the Ancillary Ligands on the Mode of Action. Inorg. Chem 2018, 57, 2851–2864. [PubMed: 29442506]
33. Esmaeilbeig A; Samouei H; Abedanzadeh S; Amirghofran Z, Synthesis, Characterization and Antitumor Activity Study of Some Cyclometalated Organoplatinum(II) Complexes Containing Aromatic N-Donor Ligands. J. Organomet. Chem 2011, 696, 3135–3142.
34. Fereidoonnezhad M; Niazi M; Ahmadipour Z; Mirzaee T; Faghih Z; Faghih Z; Shahsavari HR, Cyclometalated Platinum(II) Complexes Comprising 2-(Diphenylphosphino)pyridine and Various Thiolate Ligands: Synthesis, Spectroscopic Characterization, and Biological Activity. Eur. J. Inorg. Chem 2017, 2017, 2247–2254.
35. Samouei H; Rashidi M; Heinemann FW, Cyclometalated Platinum(II) Complexes Containing Monodentate Phosphines: Antiproliferative Study. J. Iran. Chem. Soc 2014, 11, 1207–1216.
36. El-Mehasseb IM; Kodaka M; Okada T; Tomohiro T; Okamoto K.-i.; Okuno H, Platinum(II) Complex with Cyclometalating 2-Phenylpyridine Ligand Showing High Cytotoxicity Against Cisplatin-resistant Cell. J. Inorg. Biochem 2001, 84, 157–158. [PubMed: 11330476]
37. Okada T; El-Mehasseb IM; Kodaka M; Tomohiro T; Okamoto K.-i.; Okuno H, Mononuclear Platinum(II) Complex with 2-Phenylpyridine Ligands Showing High Cytotoxicity Against Mouse Sarcoma 180 Cells Acquiring High Cisplatin Resistance. J. Med. Chem 2001, 44, 4661–4667. [PubMed: 11741483]
38. Fereidoonnezhad M; Kaboudin B; Mirzaee T; Babadi Aghakhanpour R; Golbon Haghighi M; Faghih Z; Faghih Z; Ahmadipour Z; Notash B; Shahsavari HR, Cyclometalated Platinum(II) Complexes Bearing Bidentate O,O′-Di(alkyl)dithiophosphate Ligands: Photoluminescence and Cytotoxic Properties. Organometallics 2017, 36, 1707–1717.
39. Edwards GL; Black DSC; Deacon GB; Wakelin LP, In vitro and In vivo Studies of Neutral Cyclometallated Complexes Against Murine Leukæmias. Can. J. Chem 2005, 83, 980–989.
40. Ruiz J; Cutillas N; Vicente C; Villa MD; López G; Lorenzo J; Avilés FX; Moreno V; Bautista D, New Palladium(II) and Platinum(II) Complexes with the Model Nucleobase 1-Methylcytosine: Antitumor Activity and Interactions with DNA. Inorg. Chem 2005, 44, 7365–7376. [PubMed: 16212362]
41. Ruiz J; Lorenzo J; Vicente C; López G; López-de-Luzuriaga JM; Monge M; Avilés FX; Bautista D; Moreno V; Laguna A, New Palladium(II) and Platinum(II) Complexes with 9-Aminoacridine: Structures, Luminescence, Theoretical Calculations, and Antitumor Activity. Inorg. Chem 2008, 47, 6990–7001. [PubMed: 18593114]
42. Ruiz J; Rodríguez V; Cutillas N; Espinosa A; Hannon MJ, Novel C,N-Chelate Platinum(II) Antitumor Complexes Bearing a Lipophilic Ethisterone Pendant. J. Inorg. Biochem 2011, 105, 525–531. [PubMed: 21334280]
43. Ruiz J; Rodriguez V; Cutillas N; López G; Bautista D, Acetonimine and 4-Imino-2-methylpentan-2-amino Platinum(II) Complexes: Synthesis and *In vitro* Antitumor Activity. Inorg. Chem 2008, 47, 10025–10036. [PubMed: 18844342]
44. Ma D-L; Che C-M, A Bifunctional Platinum(II) Complex Capable of Intercalation and Hydrogen-Bonding Interactions with DNA: Binding Studies and Cytotoxicity. Chem. Eur. J 2003, 9, 6133–6144. [PubMed: 14679525]
45. Omae I, Applications of Five-membered Ring Products of Cyclometalation Reactions as Anticancer Agents. Coord. Chem. Rev 2014, 280, 84–95.
46. Lalinde E; Lara R; López IP; Moreno MT; Alfaro-Arnedo E; Pichel JG; Piñeiro-Hermida S, Benzothiazole-Based Cycloplatinated Chromophores: Synthetic, Optical, and Biological Studies. Chem. Eur. J 2018, 24, 2440–2456. [PubMed: 29219223]

47. Suryadi J; Bierbach U, DNA Metalating–intercalating Hybrid Agents for the Treatment of Chemoresistant Cancers. Chem. Eur. J 2012, 18, 12926–12934. [PubMed: 22987397]
48. Liu H-K; Sadler PJ, Metal Complexes as DNA Intercalators. Acc. Chem. Res 2011, 44, 349–359. [PubMed: 21446672]
49. Zou T; Liu J; Lum CT; Ma C; Chan RCT; Lok CN; Kwok WM; Che CM, Luminescent Cyclometalated Platinum(II) Complex Forms Emissive Intercalating Adducts with Double-stranded DNA and RNA: Differential Emissions and Anticancer Activities. Angew. Chem. Int. Ed 2014, 126, 10283–10287.
50. Ruiz J; Vicente C; Haro C n. d.; Espinosa A, Synthesis and Antiproliferative Activity of a C,N-Cycloplatinated(II) Complex with a Potentially Intercalative Anthraquinone Pendant. Inorg. Chem 2011, 50, 2151–2158. [PubMed: 21314142]
51. Fereidoonnezhad M; Ramezani Z; Nikravesh M; Zangeneh J; Golbon Haghighi M; Faghih Z; Notash B; Shahsavari HR, Cycloplatinated(II) complexes bearing an O,S-heterocyclic ligand: search for anticancer drugs. New J. Chem 2018, 42, 7177–7187.
52. Samouei H; Rashidi M; Heinemann FW, A Cyclometalated Diplatinum Complex Containing 1,1′-Bis(diphenylphosphino)ferrocene as Spacer Ligand: Antitumor Study. J. Organomet. Chem 2011, 696, 3764–3771.
53. Icsel C; Yilmaz VT; Aygun M; Cevatemre B; Alper P; Ulukaya E, Palladium(II) and Platinum(II) Saccharinate Complexes with Bis(diphenylphosphino)methane/ethane: Synthesis, S-Phase Arrest and ROS-Mediated Apoptosis in Human Colon Cancer Cells. Dalton Trans. 2018, 47, 11397–11410. [PubMed: 30062356]
54. Cullinane C; Deacon GB; Drago PR; Erven AP; Junk PC; Luu J; Meyer G; Schmitz S; Ott I; Schur J, Synthesis and Antiproliferative Activity of a Series of New Platinum and Palladium Diphosphane Complexes. Dalton Trans. 2018, 47, 1918–1932. [PubMed: 29340396]
55. Albert J; Bosque R; Crespo M; Granell J; López C; Martín R; González A; Jayaraman A; Quirante J; Calvis C, Neutral and Ionic Platinum Compounds Containing a Cyclometallated Chiral Primary Amine: Synthesis, Antitumor Activity, DNA Interaction and Topoisomerase I–Cathepsin B Inhibition. Dalton Trans. 2015, 44, 13602–13614. [PubMed: 26140359]
56. Clemente M; Polat IH; Albert J; Bosque R; Crespo M; Granell J; López C. n.; Martínez M; Quirante J; Messeguer R, Platinacycles Containing a Primary Amine Platinum(II) Compounds for Treating Cisplatin-resistant Cancers by Oxidant Therapy. Organometallics 2018, 37, 3502–3514.
57. Eskandari A; Kundu A; Ghosh S; Suntharalingam K, A Triangular Platinum(II) Multinuclear Complex with Cytotoxicity Towards Breast Cancer Stem Cells. Angew. Chem. Int. Ed 2019, 58, 12059–12064.
58. Cutillas N; Martínez A; Yellol GS; Rodríguez V; Zamora A; Pedreño M. n.; Donaire A; Janiak C; Ruiz J, Anticancer C,N-Cycloplatinated(II) Complexes Containing Fluorinated Phosphine Ligands: Synthesis, Structural Characterization, and Biological Activity. Inorg. Chem 2013, 52, 13529–13535. [PubMed: 24229419]
59. Solé M; Balcells C; Crespo M; Quirante J; Badia J; Baldomà L; Font-Bardia M; Cascante M, Synthesis, Characterization and Biological Activity of New Cyclometallated Platinum(IV) Complexes Containing a *para*-Tolyl Ligand. Dalton Trans. 2018, 47, 8956–8971. [PubMed: 29922789]
60. Rocha FV; Barra CV; Mauro AE; Carlos IZ; Nauton L; El Ghozzi M; Gautier A; Morel L; Netto AVG, Synthesis, Characterization, X-ray Structure, DNA Cleavage, and Cytotoxic Activities of Palladium (II) Complexes of 4-Phenyl-3-thiosemicarbazide and Triphenylphosphane. Eur. J. Inorg. Chem 2013, 2013, 4499–4505.
61. Albert J; Bosque R; Crespo M; García G; Granell J; López C; Lovelle MV; Qadir R; González A; Jayaraman A, Cyclopalladated Primary Amines: A Preliminary Study of Antiproliferative Activity through Apoptosis Induction. Eur. J. Med. Chem 2014, 84, 530–536. [PubMed: 25063943]
62. Wilson JJ; Lippard SJ, In vitro Anticancer Activity of cis-Diammineplatinum(II) Complexes with β-Diketonate Leaving Group Ligands. J. Med. Chem 2012, 55, 5326–5336. [PubMed: 22606945]
63. Crespo M, Fluorine in Cyclometalated Platinum Compounds. Organometallics 2012, 31, 1216–1234.

64. Salwiczek M; Nyakatura EK; Gerling UI; Ye S; Koksch B, Fluorinated Amino Acids: Compatibility with Native Protein Structures and Effects on Protein–protein Interactions. Chem. Soc. Rev 2012, 41, 2135–2171. [PubMed: 22130572]
65. Fereidoonnezhad M; Ramezani Z; Nikravesh M; Zangeneh J; Haghighi MG; Faghih Z; Notash B; Shahsavari HR, Cycloplatinated(II) Complexes Bearing an O,S-Heterocyclic Ligand: Search for Anticancer Drugs. New J. Chem 2018, 42, 7177–7187.
66. Cho J-Y; Suponitsky KY; Li J; Timofeeva TV; Barlow S; Marder SR, Cyclometalated Platinum Complexes: High-yield Synthesis, Characterization, and a Crystal Structure. J. Organomet. Chem 2005, 690, 4090–4093.
67. Schneider L; Sivchik V; Chung K.-y.; Chen Y-T; Karttunen AJ; Chou P-T; Koshevoy IO, Cyclometalated Platinum(II) Cyanometallates: Luminescent Blocks for Coordination Self-Assembly. Inorg. Chem 2017, 56, 4459–4467.
68. Sakamaki Y; Ahmadi Mirsadeghi H; Fereidoonnezhad M; Mirzaei F; Moghimi Dehkordi Z; Chamyani S; Alshami M; Abedanzadeh S; Shahsavari HR; Beyzavi MH, *trans*-Platinum(II) Thionate Complexes: Synthesis, Structural Characterization, and in vitro Biological Assessment as Potent Anticancer Agents. ChemPlusChem 2019, 84, 1525–1535. [PubMed: 31943935]
69. https://dtp.cancer.gov/dtpstandard/dwindex/index.jsp.
70. Suntharalingam K; Mendoza O; Duarte AA; Mann DJ; Vilar R, A Platinum Complex that Binds Non-covalently to DNA and Induces Cell Death via a Different Mechanism than Cisplatin. Metallomics 2013, 5, 514–523. [PubMed: 23487034]
71. Armarego WLF, Purification of Laboratory Chemicals. 8th ed.; Butterworth-Heinemann 2017.
72. Hopkins JA; Lionetti D; Day VW; Blakemore JD, Chemical and Electrochemical Properties of [Cp*Rh] Complexes Supported by a Hybrid Phosphine-Imine Ligand. Organometallics 2019, 38, 1300–1310.
73. Lionetti D; Day VW; Blakemore JD, Structural and chemical properties of half-sandwich rhodium complexes supported by the bis(2-pyridyl)methane ligand. Dalton Trans. 2019, 48, 12396–12406. [PubMed: 31168559]
74. Krause L; Herbst-Irmer R; Sheldrick GM; Stalke D, Comparison of Silver and Molybdenum Microfocus X-ray Sources for Single-crystal Structure Determination. J. Appl. Cryst 2015, 48, 3–10. [PubMed: 26089746]
75. Sheldrick G, Crystal Structure Refinement with SHELXL. Acta Cryst. 2015, C71, 3–8.
76. Sheldrick G, SHELXT-Integrated Space-group and Crystal-structure Determination. Acta Cryst. 2015, A71, 3–8.
77. Morris GM; Huey R; Lindstrom W; Sanner MF; Belew RK; Goodsell DS; Olson AJ, AutoDock 4 and AutoDockTools 4: Automated Docking with Selective Receptor Flexibility. J. Comput. Chem 2009, 30, 2785–2791. [PubMed: 19399780]
78. Frisch MJ; Trucks GW; Schlegel HB; Scuseria GE; Robb MA; Cheeseman JR; Scalmani G; Barone V; Mennucci B; Petersson GA; et al., Gaussian 09, Revision A.02 2016; Gaussian, Inc., Wallingford CT.

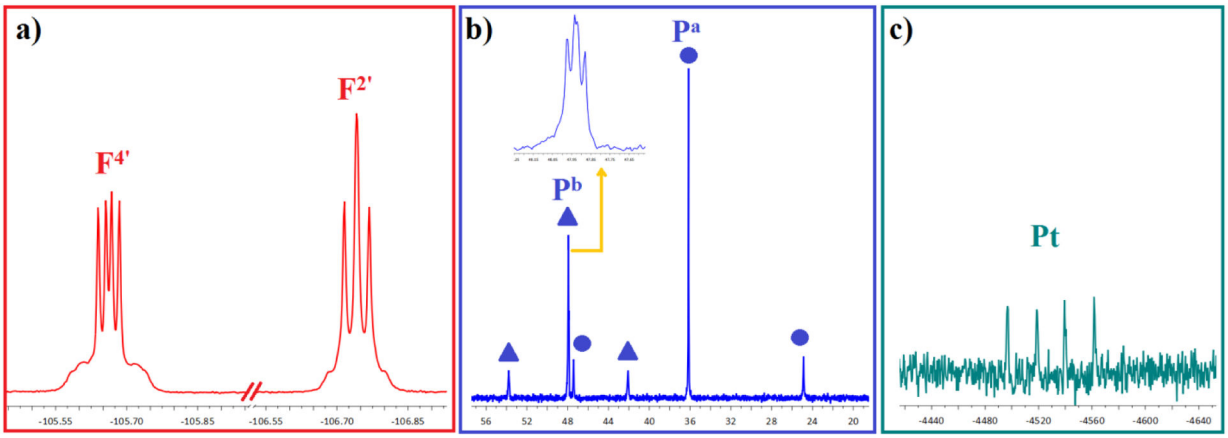

Figure 1.
a) $^{19}F\{^{1}H\}$, b) $^{31}P\{^{1}H\}$, and c) $^{195}Pt\{^{1}H\}$ NMR spectra of **3** in $CDCl_3$.

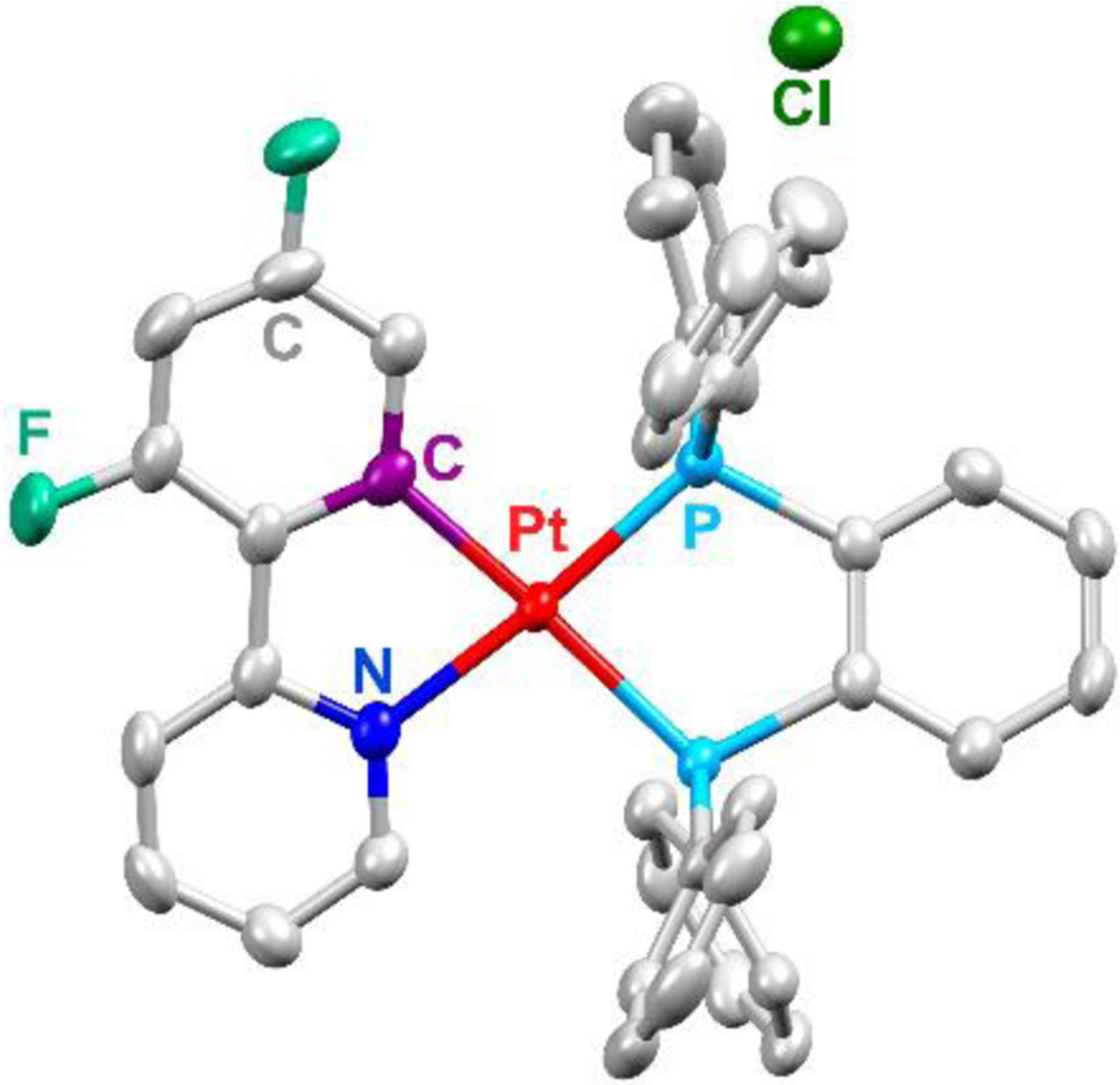

Figure 2.

ORTEP plot of **3**. Ellipsoids are drawn at the 50% probability level. Hydrogens and two CH_2Cl_2 solvent molecule have been omitted for clarity. Crystallographic data and selected geometrical parameters are summarized in Tables S1 and S2.

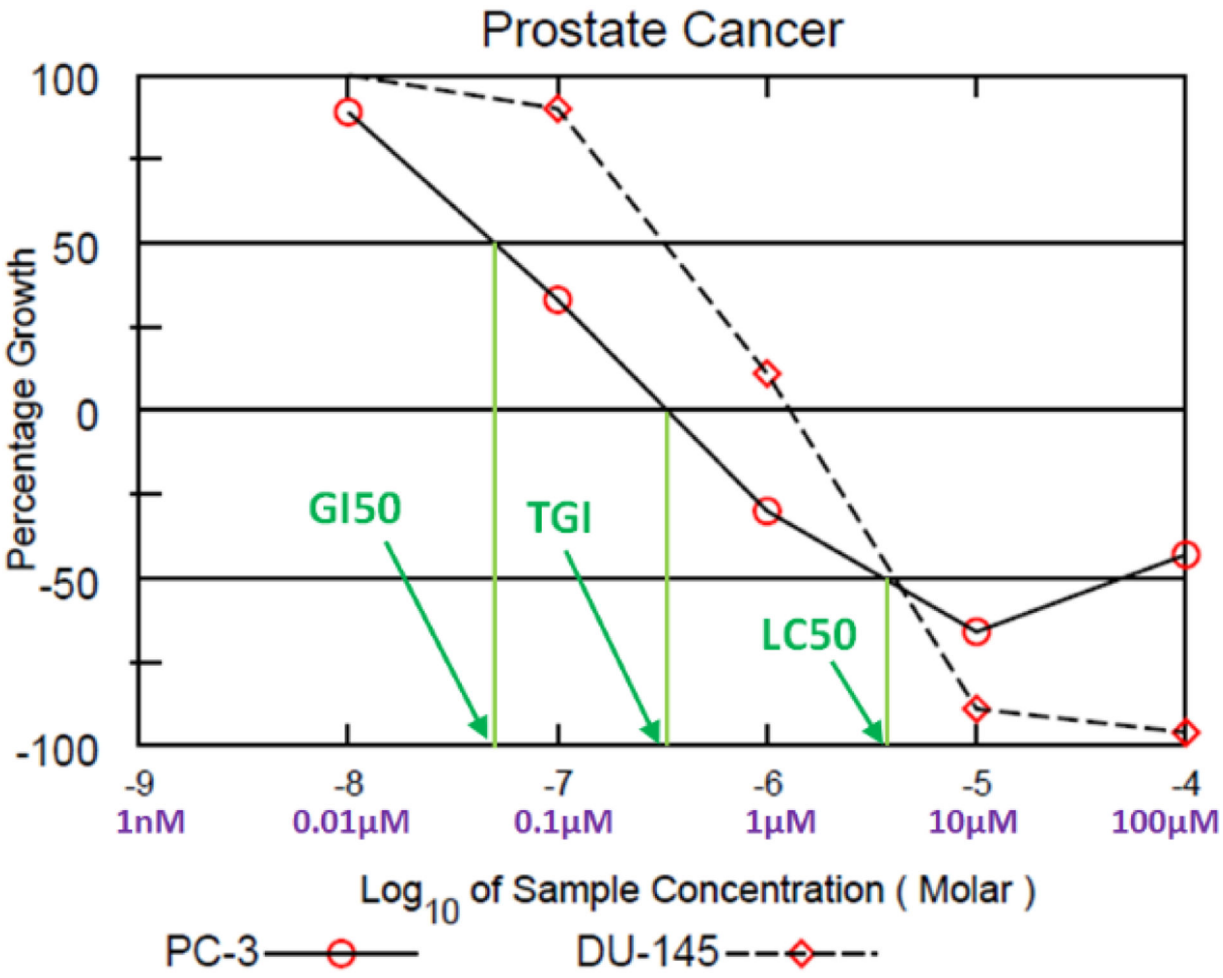

Figure 3.

Dose-response graphs for **1** assayed in prostate cancer panel, demonstrating endpoint. Data reported in µM values from NCI-60-HTCLS cell line five dose assay in 48 h continuous drug exposure protocol; GI_{50}: Growth Inhibition 50%; LC_{50}: Lethal concentration 50%; TGI: total growth inhibition.

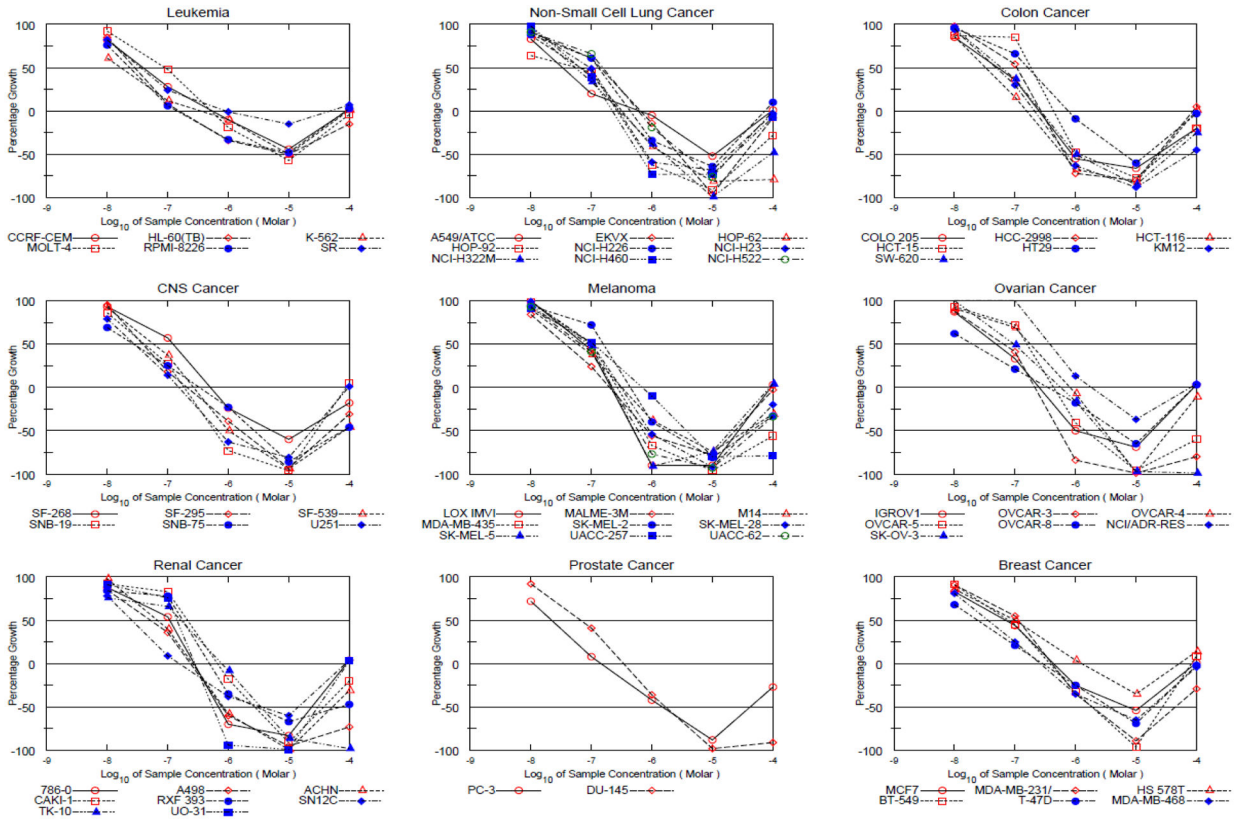

Figure 4.

Dose response curve of the results of **3** by NCI-60-HTCLS screening. 60 cell lines divided into nine sub panels at five different minimal concentrations (0.01, 0.1, 1, 10 and 100 μM).

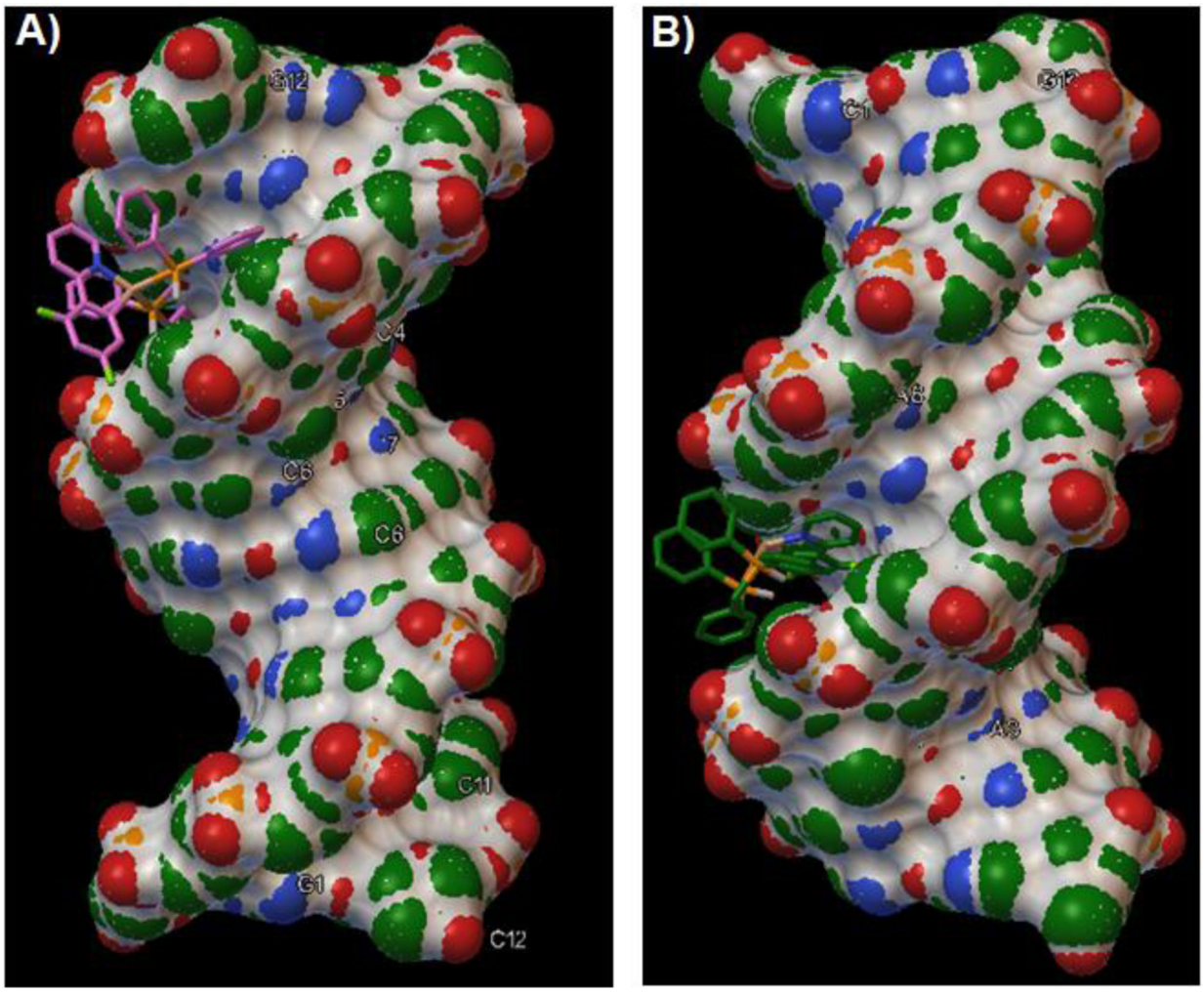

Figure 5.
Model of the interaction between (A) **1** and DNA, and (B) **2** and DNA (PDB ID: 3CO3).

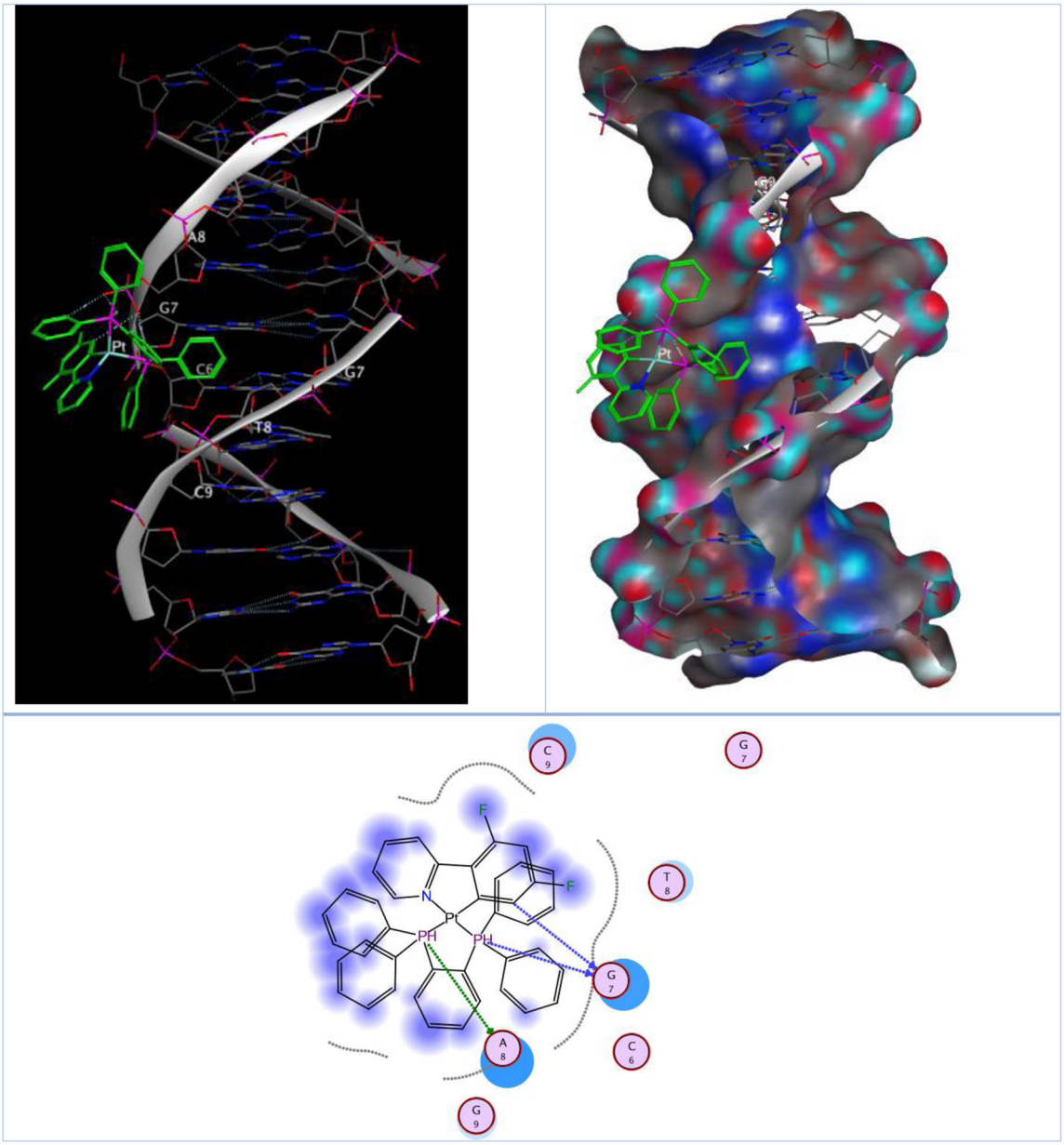

Figure 6.
Molecular docking simulation studies of the interaction between **3** and DNA (PDB ID: 3CO3).

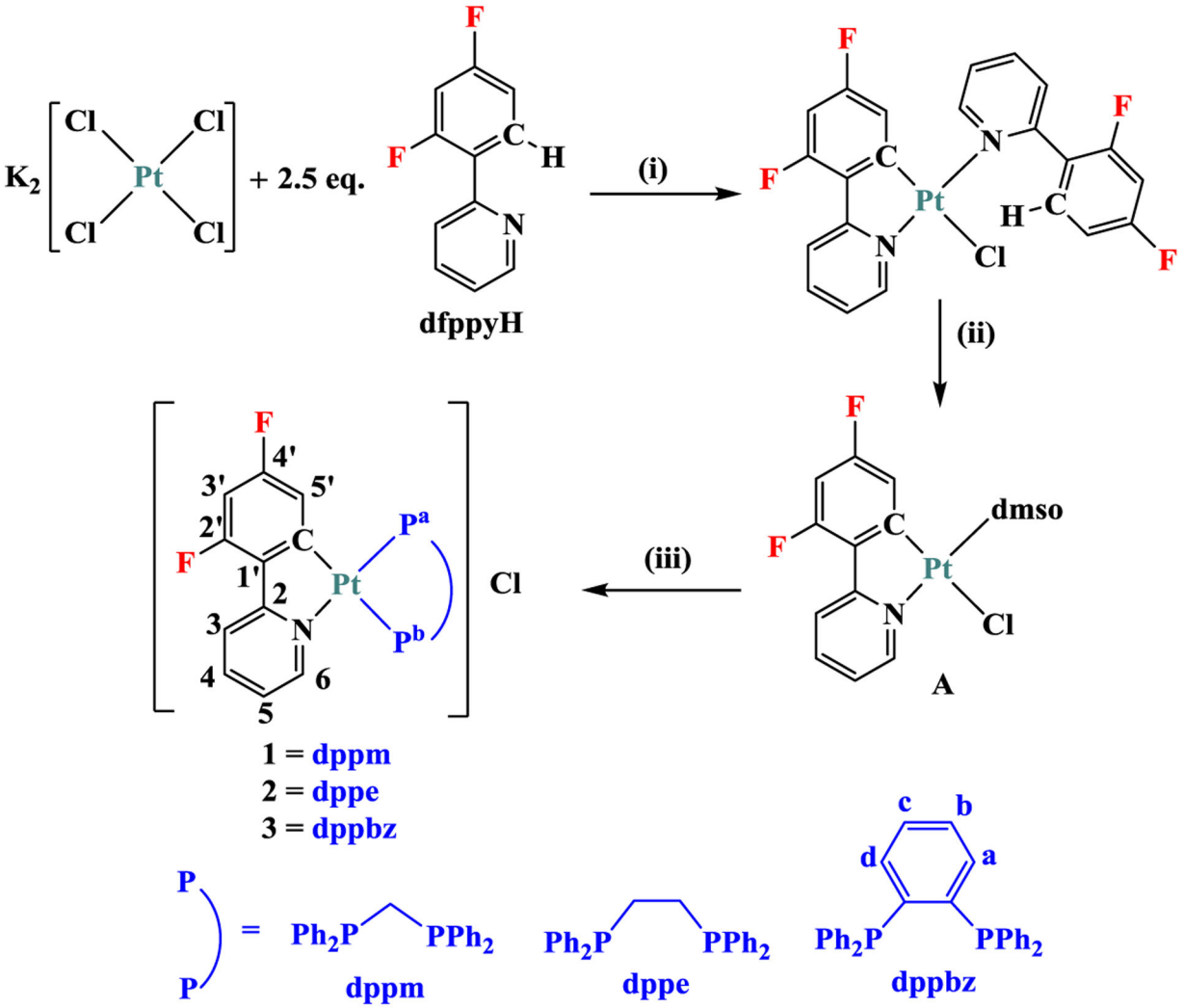

Scheme 1.

The route for the preparation of **1–3**; (i) 2-ethoxyethanol/H_2O (v/v, 3:1) at 80 °C,[66] (ii) dissolving in dmso and precipitating with H_2O,[67] (iii) 1.0 equiv. of P^P in acetone at room temperature.

Table 1.

In vitro cytotoxicity of the Pt(II) complexes against tumorigenic and non-tumorigenic cell lines.

Compound	(IC_{50} ± SD[a]) μM				selectivity index (SI)
	HeLa	SKOV3	MCF-7	MCF-10A	
1	1.759 ± 0.028	0.338 ± 0.011	0.231 ± 0.008	7.214 ± 1.261	31.229
2	1.459 ± 0.061	0.179 ± 0.003	0.061 ± 0.003	2.309 ± 0.064	37.852
3	0.135 ± 0.028	0.092 ± 0.007	0.073 ± 0.005	3.521 ± 0.210	48.233
cisplatin	17.369 ± 1.718	13.733 ± 1.085	12.372 ± 0.790	25.364 ± 0.892	2.050

[a]Values are the mean ± Standard Deviation of three independent determinations. Incubation time: 48h.

Table 2.

The mean sensitivity for complexes across all cell lines in NCI-60 screen.

		Potency in μM		
Complex	**NSC number**[a]	**Mean GI_{50}**[b]	**Mean TGI**[c]	**Mean LC_{50}**[d]
1	816001	0.195±0.041	0.490±0.131	8.32 ±1.65
2	816003	0.100±0.012	0.813±0.094	9.12±0.79
3	816002	0.069±0.008	0.347±0.107	8.13±1.05
cisplatin	119875	15.001±0.768	58.418±2.183	92.5±4.48

a: numeric identifier for substances submitted to the National Cancer Institute (NCI) for testing and evaluation.

b: 50% growth inhibition.

c: total growth inhibition.

d: 50% lethal concentration.